J. Phys.: Condens. Matter **11** (1999) 9495–9515. Printed in the UK PII: S0953-8984(99)06221-9

Magnetism in thin films

P Poulopoulos and K Baberschke†

Institut für Experimentalphysik, Freie Universität Berlin, Arnimallee 14, D-14195 Berlin-Dahlem, Germany

E-mail: bab@physik.fu-berlin.de

Received 21 July 1999

Abstract. In the last decade enormous effort has been made in research and investment to study magnetic properties of thin films because of their obvious practical applications. Coincidentally, it happens that theory has made enormous progress. *Ab initio* calculations and microscopic theories allow us for the first time in the history of magnetism to study and manipulate the magnetism on an atomic scale. In contrast to bulk magnetic materials, ultrathin films allow us to manipulate magnetism via the thickness and, by use of artificial structure growth, to produce structures which do not appear in nature. Here we discuss the fundamental magnetic observables, i.e. magnetization, Curie temperature, magnetic moment per atom, susceptibility and magnetic anisotropy, for idealized prototype thin films like Fe, Co, Ni on metal substrates such as Cu, W, Re. Finally, we present studies on trilayers, i.e. magnetic thin films separated by a spacer, like Cu. These trilayers present prototypes of interlayer coupling relevant for practical use of multilayer structures.

1. Introduction

A real avalanche in the research of thin film magnetism is currently developing. This was stimulated mainly by the major technological impact of the discovery of magnetic multilayers with (i) the easy-magnetization axis in the direction perpendicular to the film plane [1] and (ii) giant magnetoresistance (GMR) [2]. Ideally, before realizing magnetic multilayers one has to study properly their basic constituents, that are thin films in the range of a few monolayers (ML). However, this was not always possible because of the earlier lack of experimental sensitivity in the ML limit nor conclusive because of the different methods of film preparation resulting in different structures for nominally identical layers. It is only the last few years that the rapid advances of molecular beam epitaxy or other ultrahigh-vacuum- (UHV-) compatible growth techniques gave rise to films with ideal-like structure [3]. Moreover, recently, many experimental techniques have been improved in sensitivity giving information about the fundamental magnetic observables in the ML limit [4]. It is a coincidence that in parallel *ab initio* calculations have become much more powerful, e.g. [5–9]. While even before 4–5 years ago such calculations had been performed for ideal cubic lattices, recently, the real distorted structures were also taken into consideration [10, 11]. Due to pseudomorphic growth ferromagnetic ultrathin films have slightly distorted structures (1–10%) and this results in an increase of the magnetic anisotropy energy (MAE) by orders of magnitude. In terms of magnetic engineering, this means to transform soft magnets to hard magnets with large coercivities. However, MAE is still only a few tens of μeV/atom out of several eV/atom of the

† Corresponding author.

total energy. Thus, reliable results for distorted lattices demand precise input for the structural parameters down to 10^{-2} Å and, consequently, accurate studies of the structure of metallic overlayers carried out with techniques like $I(E)$-LEED became indispensable [12].

In this contribution we discuss the magnetic properties of single-crystalline films starting from the ultrathin film limit where the film thickness is smaller than the exchange length. In this limit the film behaves as an entity, as a giant magnetic molecule [13], and thus it is realistic to stay in a single-domain picture. Domain effects will appear in the present overview only in few exceptional cases. For the description of magnetization reversal mechanisms and domain-wall-related effects we refer e.g. to [14] and [15]. A complete set of experimental data will become available for better theoretical understanding only if the magnetic observables, i.e. magnetization, magnetic moment, susceptibility and MAE, are studied as a function of temperature and thickness and with full angular dependence. In section 6 we expand our review to magnetic trilayers, which are prototype systems to study multilayer magnetism. A new observable will enter our discussion, i.e. the interlayer exchange coupling J_{inter} [16]. We will engage J_{inter} and single-layer magnetism to show how the first one affects the other fundamental observables in magnetic trilayers.

In section 2 we report on experimental techniques for studying *in situ* thin film magnetism. Section 3 deals with the description of the MAE and its origin. By MAE we denote only the so-called intrinsic anisotropy and not the dipole–dipole interactions depending on the shape of the specimen. In section 4 we discuss the Curie temperature T_C and critical phenomena. In the ultrathin film limit finite-size effects reduce T_C of bulk ferromagnets in a temperature range convenient for measurements. Perpendicularly magnetized films with T_C not much higher than the room temperature are candidates for magneto-optic recording, e.g. [17]. The knowledge of T_C is then a must for optimization of properties with technological importance, since the relevant thermodynamic parameter in the analysis of MAE and magnetizations is the reduced temperature T/T_C and not the absolute temperature T. Section 5 shows ways to obtain structural information 'backward' from magnetic measurements.

2. Experimental techniques

A rather large variety of techniques are currently available to measure the magnetic properties of thin films under UHV or in the laboratory air and many of them are sensitive in the ML limit. Extended or short reviews may be found e.g. in [4, 18–22]. Here we mainly focus on two techniques, ferromagnetic resonance (FMR) and ac susceptibility measured by means of a mutual inductance (MI) bridge. They were less popular in UHV but they contributed significantly to the understanding of magnetism. We will also briefly deal with the magneto-optic Kerr effect (MOKE) and x-ray magnetic circular dichroism (XMCD).

2.1. FMR

This measures ground state magnetic properties. Its excitation energy is $\approx 1/10$ K. FMR analysis has been well established since the days of Kittel in 1949. Details for thin films may be found elsewhere [4, 20, 23]. Moreover, recently, by means of a quartz finger technique in a UHV chamber [24] *in situ* measurements with the use of large magnetic fields became available. For the present overview it is sufficient to know that a smaller external magnetic resonance field H_r means that the internal field of the ferromagnet acts parallel to H_r to fulfil Zeemann's condition, i.e. a small H_r indicates the easy-axis directions. FMR is the most suitable technique for *determining all magnetic anisotropy constants* via angular-dependent measurements [4, 20, 23]. In figure 1 we show angular-dependent measurements of the

resonance field H_r for an $(Fe_4/V_4)_{40}$ superlattice (SL) on MgO(001). The indices 4 are MLs of Fe or V in one period, while 40 is the number of SL periods. From the positions of the H_r-minima at $\theta_H = \pm 90^\circ$, figure 1(a), we conclude that the magnetization lies in the film plane. Full polar- and azimuthal-angular-dependent FMR measurements easily detect all the necessary parameters as will be discussed below. In figure 1(b) we see a small in-plane anisotropy with minima in the [100] and [010] directions. In addition a smaller asymmetry between the two ideally identical [100] and [010] directions indicates the presence of a small step-induced anisotropy [23, 25]. FMR probes the components of the g tensor and through this the orbital magnetism [26]. The FMR linewidths may serve for the characterization of the magnetic homogeneity and the structural quality of the samples [27]. The FMR intensity is a direct measure of the magnetization [28]. It was recently shown that magnetic moments of ultrathin films may be precisely determined by means of FMR [29].

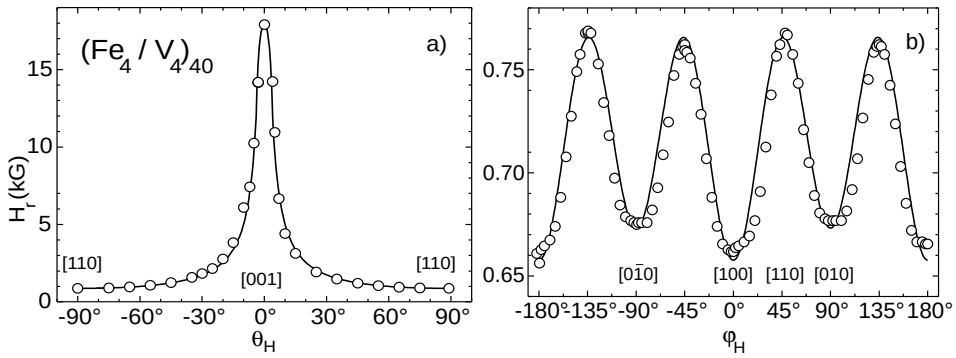

Figure 1. Angular dependences of H_r on the external magnetic field direction: (a) out-of-plane angle θ_H (from the out-of-plane[001] to the in-plane[110] axis) at $T = 10$ K and (b) in-plane angle φ_H (measured from the [100] axis) at $T = 300$ K. The solid lines are the result of a fit procedure that allows the determination of all anisotropy constants, see [23].

2.2. Ac susceptibility

The same type of quartz finger UHV chamber [24] can be used for ac-susceptibility measurements if the microwave cavity is replaced by a coil set-up operating in the frequency range 10–1000 Hz [30]. The T-dependent susceptibility $\chi(\omega) = \chi'(\omega) + i\chi''(\omega)$ is one of the fundamental observables in magnetism. It is one of the few experimental techniques investigating thin film magnetism which measures magnetic properties above T_C. Note that confusion appears in thin film literature because the most of the UHV compatible techniques, e.g. spin polarized photoemission spectroscopy, are sensitive only to the expectation value of $\langle S_Z \rangle$ whereas susceptibility measures the expectation value of $\langle S^2 \rangle$ and its fluctuations. It diverges at T_C. From the complex susceptibility the absorptive and dissipative part may be determined. The height of the χ' signal, namely χ'_{max} (in thin films it is some hundreds or thousands of SI units [31, 32]), may give geometrical information, as will be shown in section 5. Thus, it is an ideal technique for studying the T_C, critical phenomena as well as domain-related effects [33, 34].

2.3. MOKE

This is a quite common technique used in the last few years for recording hysteresis loops and temperature-dependent magnetization curves with spatial resolution [35]. A recent

development of this technique, unfortunately very little used, is the so-called ac-MOKE [36, 37] which allows us to probe χ of ultrathin films.

2.4. XMCD

This is a novel powerful technique which is based on the difference in the absorption coefficient for right and left circularly polarized x-rays in a magnetic medium (the Kerr–Faraday effect for x-rays). Both orbital and spin magnetic moments may be determined by applying the sum rules [38]. Since the technique is element specific, it is ideal for probing different magnetic elements in the same film [39]. By applying a small oscillating magnetic field it is possible to measure element-specific susceptibilities; this is ac-XMCD [40].

3. Magnetic anisotropy energy

3.1. Origin of MAE

The energy in ferromagnetic crystals which directs the magnetization along certain crystallographic axes, the easy axes of magnetization, is traditionally considered to be the magnetic anisotropy energy [41]. An easy way to demonstrate MAE is to measure the magnetization along a hard and an easy axis, as shown in figure 2. To saturate the magnetization along the hard axis a certain external field, the saturation field, has to be exceeded. The MAE is numerically equal to the area enclosed between the two magnetization curves. A simple calculation of this area in figure 2 gives for fcc Ni:

$$\mathrm{MAE} \approx (1/2)\Delta M\,\Delta B \approx (1/2)200 \times 200\ \mathrm{G}^2 = 2 \times 10^4\ \mathrm{erg\ cm}^{-3} \approx 0.2\ \mu\mathrm{eV/atom}.$$

This energy is an extremely small fraction of the total energy per atom in solids ($\approx$10 eV/atom) but all important. This fact made *ab initio* calculations of the MAE and microscopic theories for a long time impossible. This limitation, however, has left open space for treatment within the perturbation theory. Treating the spin–orbit interaction of the itinerant 3d ferromagnetic elements in a second-order perturbation theory Bruno has shown that MAE is proportional to the anisotropy of the orbital moment $\Delta\mu_L$ [42, 43], as it is known in the picture of localized magnetism, see e.g. [44]:

$$\mathrm{MAE} = \alpha \frac{\xi}{4\mu_B} \Delta\mu_L \tag{1}$$

where ξ is the spin–orbit coupling parameter [42]. In the prefactor α enter the bandwidth W and the Coulomb integral U. Since the band structure changes as a function of the thickness, W, U and α may not be constant for ultrathin films with variable thickness d. In bulk cubic crystals the high symmetry leads to near quenching of the orbital moments, $\Delta\mu_L \approx 10^{-4}\ \mu_B$/atom ($\approx$0.1 G) and consequently MAE is very small, see e.g. [45]. This difference in the orbital moment implies that the values of the saturation magnetization will be different along the easy and the hard axis, as demonstrated in the inset of figure 2. Strictly speaking, the saturation magnetization in bulk ferromagnets like Fe, Co, Ni is not a simple scalar magnitude but depends on the orientation of the crystallographic axes, i.e. the total moment/atom (including orbital and spin as well as sp contributions) depends on the crystallographic orientation.

In ultrathin films and multilayers the situation is quite different. Two main reasons give rise to symmetry deviations that lift partially the quenching of the orbital moment and increase MAE by orders of magnitude: (i) the reduced symmetry at the surfaces,

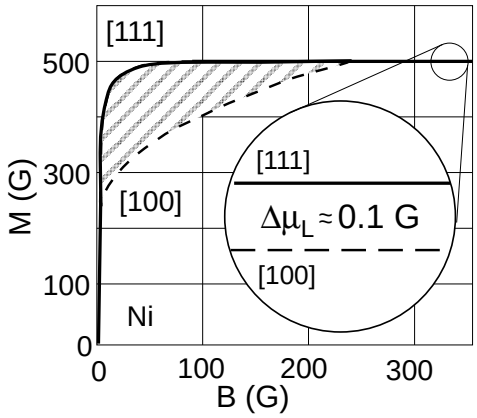

Figure 2. Magnetization curves for the easy [111] and hard [100] axes of bulk Ni [41]. The area enclosed between the two curves is a direct measure of MAE. The values of the magnetization along the easy and hard axes are slightly different due to equation (1) (inset).

interfaces or atomic step edges resulting in a surface energy contribution K^S, first recognized by Néel [46], see also [21, 47]; (ii) the distortion of the lattice due to strain between the magnetic layers and the substrate or the non-magnetic layers, in the case of multilayers, resulting in a volume energy contribution K^V, see e.g. [45, 48]. Unfortunately, in thin film literature mostly the first (Néel's) argument has been discussed to describe MAE in thin films. Even in very recent literature it was assumed that the middle part of thin films behaves like the bulk material, i.e. K^V has the bulk values. It is one of the focal points of this review that pseudomorphic growth of a ferromagnet on certain substrate materials changes the crystal structure by a few hundredths of an Å and, consequently, this increases MAE by orders of magnitude! This second effect can be manipulated by growth conditions (temperature, substrate) whereas the surface contribution is almost independent of the substrate material. E.g. K^S values of Ni grown on W(110) and Cu(001) are almost equal whereas K^V is very small for W(110) and two orders of magnitude larger for Cu(001) [49]. Only the surface contribution K^S/d is thickness dependent, as the following equation suggests [21]:

$$K = K^V + 2K^S/d. \tag{2}$$

A thin film has usually two different surfaces: an interface with the substrate and a real surface facing vacuum. These two K^S contributions are definitely different. Moreover, in some sense a real surface may extend to the second layer. For simplicity we adopt the commonly used notation of the prefactor '2' in equation (2), but caution has to be taken if one starts to interpret the numerical value of K^S. In many cases K is not a linear function of $(1/d)$. A change of the slope occurs at a certain thickness where relaxation of the strain starts. This is shown in figure 3 for Ni/Cu(001). Note that the data of figure 3 are presented at two constant reduced temperatures in order to give reliable information. It was demonstrated recently that Co/Cu(111) films if analysed not at a constant reduced temperature may give erroneous results concerning the sign of K^S [50].

Besides MAE, another source of anisotropy becomes important to thin films. This originates from long-range dipolar interactions between the moments and thus it is strongly dependent on the shape of the specimens (shape anisotropy $2\pi M^2$). In many thin films shape

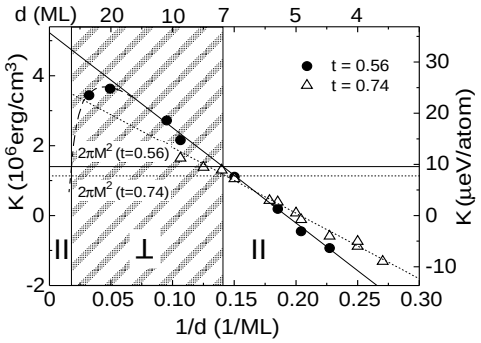

Figure 3. K as a function of $1/d$ for two reduced temperatures t [45, 66]. The marked area is the perpendicularly magnetized phase where the intrinsic anisotropy exceeds the shape anisotropy.

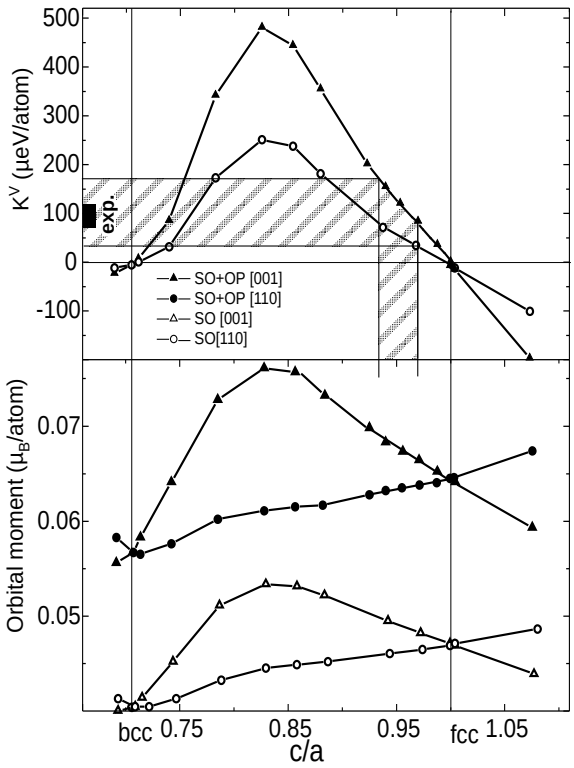

Figure 4. *Ab initio* calculations of (a) the volume anisotropy and (b) the orbital moment as a function of the axial ratio c/a for fct Ni/Cu(001) [10]. Results are presented with only spin–orbit (SO) or SO plus orbital polarization (OP) (see text). Both anisotropy and orbital moment increase significantly due to the tetragonal distortion. The orbital moment is larger along the easy axis.

anisotropy dominates and it favours a different easy axis than the intrinsic MAE. For Ni/Cu(001) in figure 3 we see that the total intrinsic MAE K is smaller than $2\pi M^2$ below $d \approx 7$ ML and thus it favours the easy-axis to be in plane. For thicker films the large positive intercept with the y-axis ($K^V \approx 30$ μeV/atom) overcomes $2\pi M^2$ favouring an out-of-plane easy axis [51].

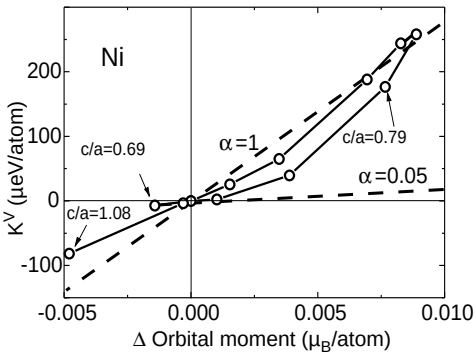

Figure 5. Calculations for the change of volume anisotropy and orbital moment with the ratio c/a [10]. The straight line corresponds to predictions of equation (1). Obviously there is not strict proportionality between MAE and $\Delta\mu_L$.

However, equation (1) and experiments by XMCD [52, 53] or FMR [26] support the argument that the larger orbital moment lies always along the intrinsic easy axis, i.e. the one determined exclusively by MAE.

The successive evolution of *ab initio* methods have increased the accuracy of calculations of MAE. It is a challenge that for the first time the last few years' calculations yield reasonable values for MAE, that is comparable to the experimental ones [8–10]. In figure 4 we may see calculations for (a) K^V and (b) orbital moment for face-centred tetragonal (fct) Ni versus the axial c/a-ratio at $T = 0$ K [10]. The calculations were carried out within the framework of the linearized muffin-tin orbital method [54] with or without the orbital polarization correction suggested by Eriksson *et al* [55]. A huge increase of both K^V and μ_L is obtained for deviations from the cubic fcc and bcc symmetry. A small tetragonal distortion of the order of 0.02 Å results in $K^V \approx 100$ μeV/atom!, in excellent agreement with the experiment [51]. From figure 4 one is able to plot directly the anisotropy energy as a function of the anisotropy of the orbital moment with implicit parameter the c/a-ratio, shown in figure 5. We see immediately that K is not a linear function of $\Delta\mu_L$. It may be approximated by a linear function as shown by the two dashed lines with $\alpha = 1$ or $\alpha = 0.05$. Obviously, there is not a strict proportionality between MAE and $\Delta\mu_L$. This conclusion is verified by other recent *ab initio* calculations [56, 57] and suggests that the prefactor in equation (1) is rather a function of $\Delta\mu_L$ than a simple numeric constant. As a result, MAE cannot be determined by measuring $\Delta\mu_L$.

3.2. Higher order anisotropies, temperature dependence and spin reorientations

As said before in the history of bulk magnetism MAE was treated as a phenomenological quantity of the free energy density E [45, 58]. Commonly E is expanded in powers of trigonometric functions or Legendre polynoms. This expansion in second, fourth and sixth order is of some interest because it describes very nicely the local symmetry as can be seen in figure 1(b), where the fourfold in-plane anisotropy is superimposed by a twofold symmetry originating from steps in thin films. Keeping up to fourth order terms of K_i and including shape anisotropy the E of an fct film is written:

$$E = 2\pi M^2 \cos^2\theta - K_2 \cos^2\theta - \tfrac{1}{2}K_{4\perp}\cos^4\theta - \tfrac{1}{2}K_{4\parallel}\tfrac{1}{4}(3 + \cos 4\phi)\sin^4\theta. \tag{3}$$

K_i are the anisotropy constants and have surface (thickness-dependent) and volume (thickness-independent) contributions according to equation (2). K_4 describes the fourfold symmetry but

no cubic symmetry *per se*; in most thin films $K_{4\perp} \neq K_{4\parallel}$. This is shown clearly in figure 6 where K_2 and K_4 of (a) 7–8 ML Ni/Cu(001) and (b) a $(Fe_2/V_5)_{60}$ SL are plotted as a function of temperature. In both cases $K_{4\parallel} < K_{4\perp}$; furthermore we show that K_4 is not always a small higher order correction in the MAE; in contrast $K_{4\perp}$ and K_2 (here $K_{2\perp}$) are of the same order of magnitude.

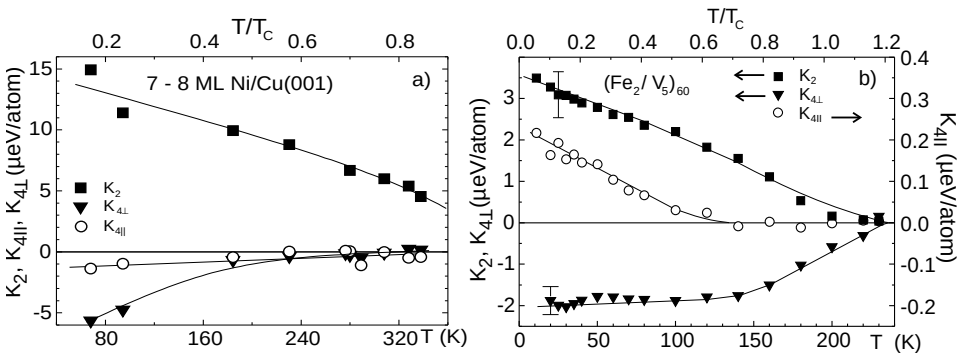

Figure 6. K_2 and K_4 determined by FMR for (a) ultrathin 7–8 ML Ni/Cu(001) films [49] and (b) Fe_2/V_5 superlattices [26]. Note that K_4 is comparable to K_2 and $K_{4\parallel} \neq K_{4\perp}$, as a result of the tetragonally distorted structures.

In our convention positive K_2 favours out-of-plane anisotropies. Positive K_2^S or K_2^V compete with shape anisotropy and they may result in a thickness-dependent switch of the easy magnetization axis (spin-reorientation phase transition—SRT) [45, 59]. In most Fe and Co-based systems $K_2^S > 0$ driving the magnetization out of the film plane for small film thicknesses [60]. However, in Ni-based films the situation is reversed: $K_2^S < 0$ and the only source of perpendicular magnetization is $K_2^V > 0$. This gives rise to a SRT from in to out of plane at 7–8 ML Ni/Cu(001) [51] and a unique Pt-thickness-dependent SRT in Ni/Pt multilayers [61]. Fourth order anisotropies are extremely important near SRT: they are the dominant terms determining the order of the reorientation [49, 62, 63]. At the SRT higher order anisotropies may stabilize tilted magnetization configurations [49, 62–65]. The equilibrium angle of the magnetization may be calculated as a function of K_2, K_4 and M, e.g. [49, 63].

Magnetic anisotropies are temperature-dependent quantities [58], as experimentally illustrated in figure 6. Magnetic anisotropies of itinerant ferromagnets vanish at T_C, see figure 6(b), also [66]. However, there are well known examples, like Gd, where finite anisotropies (single-ion MAE) may be present at higher temperatures than the T_C; theoretical models of single ion anisotropies describe successfully this effect [67, 68]. The different temperature dependence of surface, volume and shape anisotropies may give rise to SRTs as a function of temperature. Such reorientations have been observed in many Fe-based films. The films are out-of-plane magnetized at low temperatures, then they usually enter a multidomain configuration and finally, at higher temperatures, the magnetization turns in plane [69–72]. While these SRTs are consistent with entropy-based argumentations [73], a striking anomalous SRT from in (low temperatures) to out of plane (high temperatures) has been recently observed in Ni/Cu(001) [74]. This is demonstrated in figures 7(a)–(d). For low temperatures a small H_r is measured with H in plane (easy axis); for high temperatures a small H_r appears for H normal to the film plane. Most important are stable minima in H_r for intermediate temperatures: these indicate a continuous rotation of the easy axis [75]. Experimentally this SRT is now well understood via the different temperature dependences of surface, volume and shape anisotropies [74]. Calculations based on mean-field and perturbation theory [76]

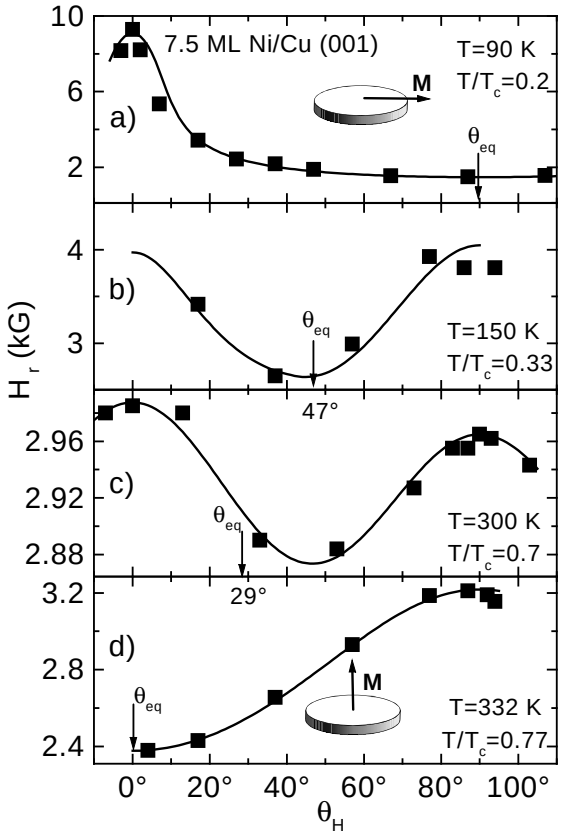

Figure 7. Angular-dependent H_r values as a function of the angle θ_H between the applied field H and the film normal [001] with increasing temperature (from (a) to (d)) provide a direct evidence of the anomalous and continuous SRT in ultrathin Ni/Cu(001) films [75]. θ_{eq} is the angle of the magnetization at equilibrium with respect to [001].

or the Hubbard model [77] have managed to describe successfully this SRT. The systematic FMR study of the magnetic anisotropies as a function of thickness and temperature has led to the production of the magnetic phase diagram of Ni/Cu(001), figure 8. The solid line is the finite-size scaling and we will deal with it in the next section. In the area between in-plane and out-of-plane ferromagnetism solid triangles up (down) correspond to complete $\perp$ ($\|$) orientation and the open circles and squares to the tilted configurations. Figure 8 renders Ni/Cu(001) as one of the most complete systems in the study of ferromagnetism in the ultrathin film limit.

4. T_C and critical phenomena

4.1. Finite-size effects

Bulk ferromagnetic materials or thick films have well defined T_C values depending exclusively on their composition [41]. However, as the film thickness approaches the ultrathin limit and since the correlation length ξ diverges at T_C, the correlated fluctuating magnetic moments in a volume ξ^3 (Kadanoff block) are influenced by the finite size of the specimen. The T_C is then

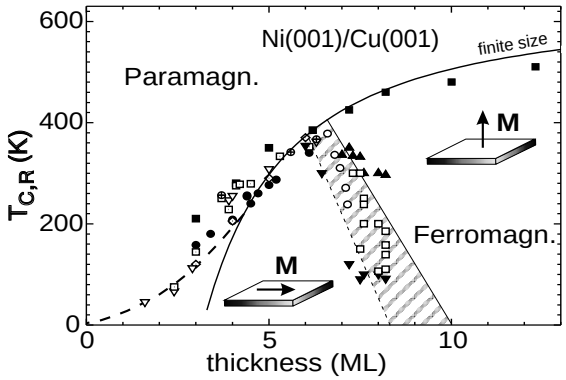

Figure 8. Magnetic phase diagram for Ni/Cu(001) for thicknesses up to 12 ML [62]. The lines separate ferro- from paramagnetic and in- from out-of-plane magnetized states. SRTs may be observed as a function of increasing thickness or increasing temperature, both in the sense in→out of plane.

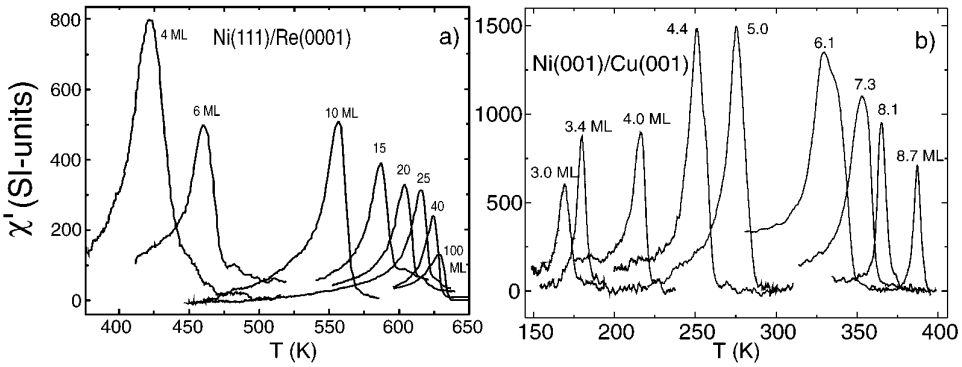

Figure 9. Calibrated in-phase susceptibility by MI versus temperature for several thicknesses of (a) Ni(111)/Re(0001) [79] and (b) Ni/Cu(001) [32]. Note that the susceptibility is three orders of magnitude larger than that of a perfect diamagnet. Such large susceptibilities have never been observed in bulk ferromagnets.

reduced as observed for the first time for Ni(111)/Re(0001) [78]. This effect is illustrated for Ni(111)/Re(0001) [79] and Ni/Cu(001) [32] in figures 9(a) and (b), respectively. One may clearly see that the χ'_{max} shifts towards lower temperatures when d decreases and it is very large: $\chi'_{max} \approx$ 800–1500 SI units. Monitoring *in situ* noise-free χ of ultrathin Ni films in the ML limit is a great challenge, taking into account that $\chi \propto \mu^2$ and the Ni moment is about 12 times smaller than that of Gd where previous susceptibility measurements have been performed [30]. In case of Ni/Cu(001) only in-plane magnetized films (up to about 8 ML) could be measured. Thicker films are perpendicularly magnetized and they do not present measurable susceptibility peaks at T_C [33, 34]. On the other hand, the lower limit of 3 ML was determined only by the lowest accessible temperature in the UHV chamber. Note that even 1.6 ML Ni/Cu(001) was found by XMCD to be ferromagnetic with $T_C = 46$ K [80].

4.2. Effect of capping and substrate on T_C

The majority of experiments on ultrathin films are performed not in UHV but on samples protected by a non-ferromagnetic capping layer. Thus, caution is needed if one discusses their properties and compares to theoretical calculations carried out for uncapped films. Table 1 shows the T_C values of Ni and Co in-plane magnetized ultrathin films on Cu(001) before and after capping with Cu. T_C values were determined by susceptibility measurements or XMCD remanent magnetization curves. In all cases a reduction in T_C is observed after capping, see also [81–83]. The effect is practically saturated even before the completion of evaporation of 1 ML of the capping layer; compare, for example, the reduction of the T_C after only 0.5 ML Cu-capping layer (fifth row) to the other ones. Note the stronger effects of capping in the T_C of Co films, which is reduced by about 100 K. This is possibly related to the smaller thickness of Co compared to Ni. Indeed, theoretical calculations suggest that the additional interface results in a reduction of the magnetic moments through hybridization effects [84] and, consequently, T_C is reduced. Our susceptibility data support this argumentation since we observe that the T_C reduction after capping is accompanied by a reduction of χ'_{max}. Thus, the T_C of 2 ML Co which has only magnetic layers in proximity to Cu should be much more affected than that of 4–6 ML of Ni. The effects of the first (to the substrate) or the second (to the capping layer) interface could make real T_C values very different from the calculated ones for free standing magnetic monolayers [85].

Table 1. T_C of various ultrathin Ni and Co on Cu(001) films before capping with Cu. The capping layer thickness and the decrease ΔT_C after capping are noted. ΔT_C is more pronounced in the case of $d \approx 2$ ML Co films.

$d_{ferromagnet}$ (ML)	T_C (K)	d_{Cu} (ML)	ΔT_C (K)
Ni 3.6	168	2.0	−31
4.0	217	2.5	−37
4.0	210	3.5	−50
5.0	275	2.0	−25
5.1	278	0.5	−23
5.1	263	7.0	−28
Co 1.9	290	6.8	−120
1.8	300	4.8	−75

4.3. Critical behaviour

At the phase transition from ferro- to paramagnetism the order parameter, the spontaneous magnetization, vanishes following a power law of the form:

$$M(T) = M(0)(1 - T/T_C)^{\beta} \tag{4}$$

where β is a critical exponent ranging between 1/8 and 1/2 depending on the dimensionality in spin and real space, the model of calculation and the anisotropy. Determination of critical exponents may be done only provided that T_C is accurately determined. However, it was shown [86] that small uncertainties in T_C may result in erroneous conclusions. The best way is not to fit the $M(T)$ curve with both T_C and the exponent β as parameters, but to determine T_C in a separate experiment and then to evaluate β from the fit of $M(T)$. Moreover, the decision about the order parameter might not be trivial. Usually the remanent magnetization, instead of the spontaneous one, is the measurable order parameter and T_C is considered to coincide with the temperature where M_r vanishes [87]. However, for perpendicularly magnetized samples

this was shown not to be appropriate because of domain effects [33, 34]. A better choice for the order parameter in this case seems to be the magnetization under a small applied field [33, 88]. When β is properly determined, one of the most striking experiments is to search for dimensionality crossovers by reducing d. In Figure 10 the linewidth ΔH of FMR is plotted as a function of temperature and film thickness for Ni(111)/W(110) [89]. The relatively low T_C and the immiscibility between Ni and W make these films ideal candidates for studying critical phenomena. Spin fluctuations near T_C give rise to a considerable increase of ΔH. In the inset of figure 10, β is shown as a function of d. The change of β-values at 6 ± 1 ML indicates unambiguously a dimensional crossover between 2D and 3D.

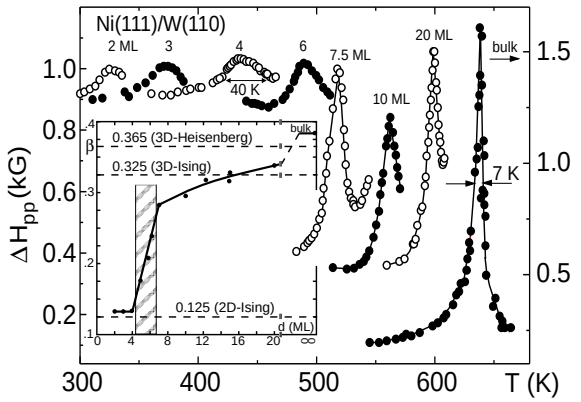

Figure 10. FMR linewidths ΔH with temperature for Ni(111)/W(110) films 2–20 ML thick. Note the pronounced increase at about 6 ML resulting from a change of the dimensionality. In the inset, the critical exponent β switches at this thickness from values consistent with 2D to 3D models describing ferromagnets [89].

5. Correlation between magnetism and structure

Structural characterization techniques like $I(E)$-LEED [12, 90] or scanning tunnelling (STM) [91] and electron microscopies [92] have been significantly evolved in the last few years, facilitating in many cases the interpretation of magnetic properties of thin films. Here, however, we will present interesting cases which allow the opposite, i.e. the determination of structure from magnetic observables. For example, in figure 3, as long as $K(1/d)$ remains linear there is no structural change of the films with d. This conclusion has been verified by recent $I(E)$-LEED experiments [12]. $K(1/d)$ departs from linearity (at $d \approx 15$ ML) when the structure starts to relax from the fct to the fcc with smaller anisotropy [51].

χ'_{max} may give structural information. While the internal susceptibility equals $\chi'_{loc} = \partial M/\partial H_{loc}$, the measured signal χ'_{exp} is limited by the demagnetizing factor N:

$$\chi'_{exp} = \frac{1}{1/\chi'_{loc} + N}. \tag{5}$$

Taking into account that χ'_{loc} diverges at T_C, equation (5) determines the measured susceptibility to be $\chi'_{exp} \leqslant 1/N$. It is not sufficient to apply the continuum model in which the demagnetizing factor parallel and perpendicular to the film plane is $N_\parallel = 0$ and $N_\perp = 1$, respectively. For thin plates with finite diameter D one obtains $N_\parallel \approx \pi d/4D$. By measuring χ'_{exp} we can deduce, via equation (5), a lower limit for the lateral size of magnetically homogeneous regimes.

In figure 8, for example, where $\chi'_{exp} \approx 10^3$, one may deduce that Ni samples of thickness $d \leqslant 1$ nm have a homogeneous magnetic response over a lateral size of about 1 μm! This principle was applied in the case of 11 ML Gd/W(110) films and resulted in $D \approx 0.5$ μm [93, 94]. A successive UHV-STM study has proven that indeed this was the correct island size of such Gd/W(110) films [95].

4 ML Fe/Cu(001) experience a reversible structural transformation between fct and fcc as a function of temperature [96]. At the transition temperature T^*, fcc and fct phases coexist and it was believed that the fct structure was located only on the surface layer. However, a careful FMR analysis has shown that this model has to be reconsidered [97]. In figure 11(a) one may see that the FMR intensity of 4 ML Fe/Cu(001) vanishes at 320 K, like the MOKE signal in [96], which corresponds to T^*. The transformation seems to be completely reversible. However, one cannot safely conclude that T^* is the ordering temperature. The anisotropy field measured by FMR [97] does not vanish at T^*. One may see in figure 11(b) that K_2 has a gradual variation in the neighbourhood of T^*. The smooth variation of K_2 at T^* indicates that the structure changes from fct to fcc through volumina that shrink with temperature (inset of figure 11(b)). Moreover, no dramatic increase of the FMR linewidths was observed [97] as one would expect (see e.g. figure (10) if T^* corresponds to T_C. A rough estimation via the coherence of spin waves determined a minimum size of magnetic homogeneous regimes in the range 50–80 nm [97]. The model of fct domains of figure 11 was also supported by the analysis of the coercivities of such ultrathin Fe/Cu(001) films [98].

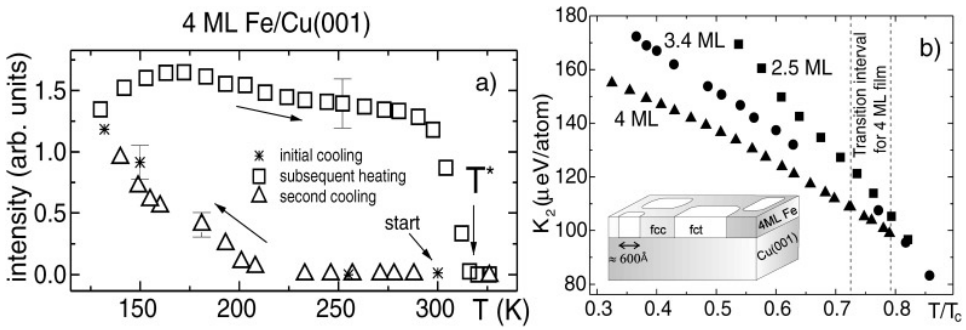

Figure 11. Temperature dependence of (a) the FMR intensity (proportional to the magnetization) for 4 ML Fe/Cu(001) and (b) K_2 for 2–4 ML Fe/Cu(001). No significant change of K_2 is observed at the transition temperature T^* for the 4 ML Fe/Cu(001) film. The inset of (b) illustrates the structural model compatible with our magnetic observations at T^* [97].

Another example of deducing structural information from magnetism is the case of the T_C jump at the coalescence of Co islands on Cu(001). Figure 12 shows the T_C of Co/Cu(001), determined with various techniques, in the thickness range 1–2.5 ML. T_C exhibits a pronounced discontinuity at $d \approx 1.8$ ML. This is attributed to the coalescence of double layered Co islands and it is in excellent agreement with UHV-STM images [99]. At 1.8 ML T_C is strongly metastable and it varies strongly with time and heat treatment. Interestingly, below 1.8 ML the system presents ferromagnetic behaviour as demonstrated via MOKE hysteresis loops and non-zero XMCD signals at remanence. Superparamagnetic behaviour was moreover excluded by simple calculations showing that the blocking temperature that corresponds to the STM-determined island size of Co ($\approx$5 nm) is only a few K, while hysteresis is exhibited at temperatures of the order of 100–200 K [100].

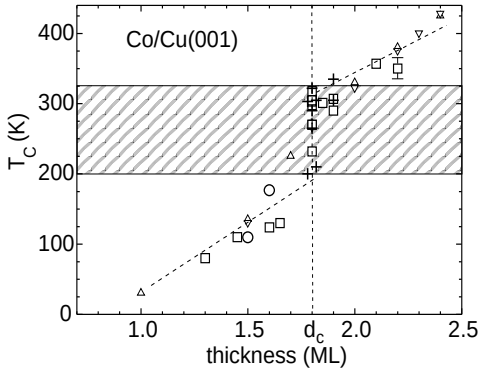

Figure 12. T_C of Co/Cu(001) as a function of the film thickness. A steep increase of T_C (T_C-jump) occurs at the coalescence of Co islands at $d \approx 1.8$ ML. Different symbols correspond to different techniques of T_C determination: XMCD (squares), MOKE (circles), MI ac-susceptibility (crosses), while triangles are values from other experimental groups. Details may be found in [100].

6. Magnetic trilayers: a prototype for interlayer coupling (J_{inter})

Magnetic layers interact through non-magnetic spacers via the so-called interlayer exchange coupling. Theoretical approaches based on the Ruderman–Kittel–Kasuya–Yosida (RKKY) model, quantum well states etc are now available for its description [16, 101]. The technological impacts, mainly of the magnetotransport properties (GMR effect), are also discussed in detail elsewhere [102, 103]. However, little work was done on the relation between J_{inter} and other fundamental magnetic observables on a temperature-dependent basis, see e.g. [104]. It is the aim of this part to address and elucidate the following questions: do coupled magnetic layers present separate or a single (common) T_C? How does J_{inter} affect the temperature-dependent sublayer magnetizations and susceptibilities? For this purpose we use prototype-like trilayers with Co (1.5–3 ML) and Ni (3–5 ML) sublayers with ideal-like single crystalline structure. These layer thicknesses were selected in order to bring T_C into a convenient temperature range for measurements without interdiffusion problems.

6.1. Do coupled films present two T_Cs?

In the following we present mainly data recorded by the XMCD technique. The beauty of this technique is its element specificity. Thus, we can probe separately the Ni and Co magnetizations in a trilayer. In figure 13(a) we see the XMCD spectra at the $L_{2,3}$ edges of Ni and Co in a Co/Cu/Ni/Cu(001) trilayer at 290 and 336 K. Co and Ni XMCD spectra at 290 K reveal ferromagnetism in both layers (dotted lines). However, at 336 K Co still has non-zero XMCD signals, while, within our experimental resolution, Ni shows no ferromagnetic response (solid lines). That is, Ni has entered the paramagnetic phase. In figure 13(b) the temperature dependence of the remanent magnetizations of both Ni and Co are presented near the temperatures of interest. It is clearly shown that Ni shows no ferromagnetism above $T_C^{*\,Ni} = 308$ K. The T_C of Co was found to be about 340 K. These measurements show that, despite the very thin Cu spacers allowing a strong interlayer coupling between Co and Ni, the two layers enter the paramagnetic phase at different temperatures.

If the temperature T_C^{*Ni} corresponds to a second T_C of the trilayer, one would expect to see two susceptibility maxima in these trilayers. We did study several trilayers with various Cu spacers recording a single χ'_{max} at the temperature where the Co magnetization vanishes [105].

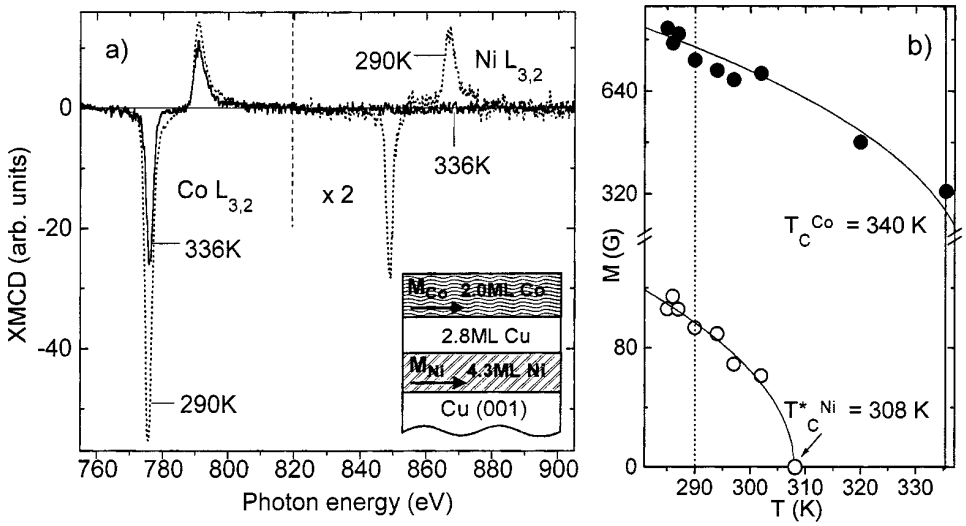

Figure 13. (a) XMCD spectra at the $L_{2,3}$ edges of Xi and Co at 290 (dotted) and 336 K (solid lines). (b) Temperature dependent remanent magnetizations for the Ni and Co layers in the same trilayer. No ferromagnetic response for Ni could be recorded above 308 K.

This corresponds to the T_C of the trilayer. Our observation is in agreement with theory: in a strict thermodynamic sense the coupled system should exhibit only one true phase transition at the temperature where the higher T_C element (here it is Co) is placed [106]. Only for thicker Cu spacers ($d_{Cu} \approx 25$ ML), where J_{inter} is very small, is a second χ'_{max} observed at T_C^{*Ni}, as shown in figure 14 [105]. This second χ'_{max} at T_C^{*Ni} does not correspond to a phase transition. It may rather be characterized as a susceptibility resonance [105]. That is, there is a resonant fluctuation of Ni spins at a temperature of about 250 K where the Co spins are still ferromagnetically aligned. Ac-susceptibility is strongly suppressed by minute values of J_{inter} (≈10–100 neV/atom!); thus it may serve as a sensitive probe of the interlayer coupling [107].

6.2. Effects of J_{inter} on T_C^{*Ni}

The XMCD technique may also probe the sign of the interlayer coupling. Note in figure 15 the difference of the sign of Ni spectra in trilayers with Cu spacers of different thickness. From these spectra J_{inter} is determined to have the opposite sign in the two trilayers [108]. The observation of antiferromagnetic (AFM) coupling in trilayers with such thin Cu spacers guarantees that the physics is dominated by the interlayer coupling and not pinhole problems [109]. Besides the coupling sign, the XMCD spectra have allowed the determination of the Ni and Co spin and orbital magnetic moments in trilayers. More details for this interesting subject may be found in [110].

Figure 16 depicts element-specific remanent magnetization curves for Ni and Co in bi- and trilayers. The Ni magnetization in the bilayer (open circles) vanishes at a temperature of about 270 K which corresponds to the temperature T_C^{Ni}, since Ni is in-plane magnetized [87]. After the deposition of Co on the top of the Cu/Ni bilayer the temperature T_C^{*Ni} where the Ni magnetization (closed circles) vanishes is increased by $\Delta T_{Ni} \approx +40$ K. The Co magnetization (closed diamonds), on the other hand, vanishes at much higher temperatures. The increase in the temperature where the Ni magnetization vanishes could be understood, in a first approximation

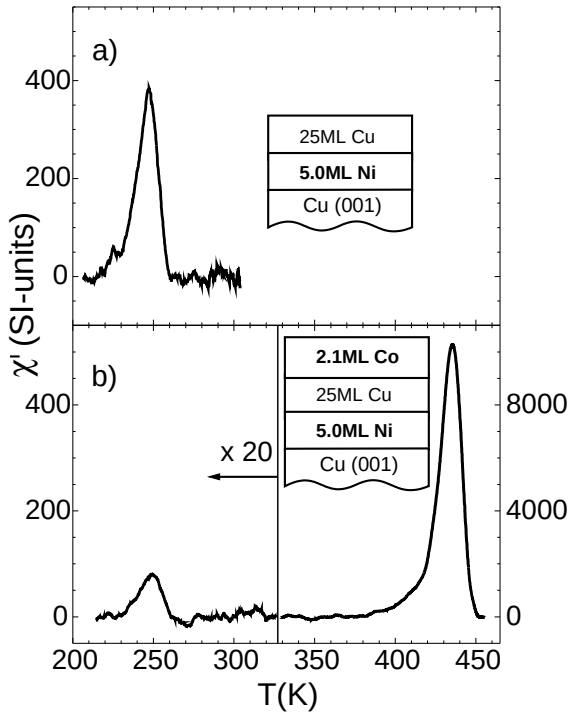

Figure 14. Susceptibility signals by MI for (a) 5 ML Ni capped with Cu and (b) Co/Cu/Ni trilayer [105]. Note the presence of two susceptibility maxima in one trilayer. The signal at the lower temperature is suppressed due to the interlayer coupling.

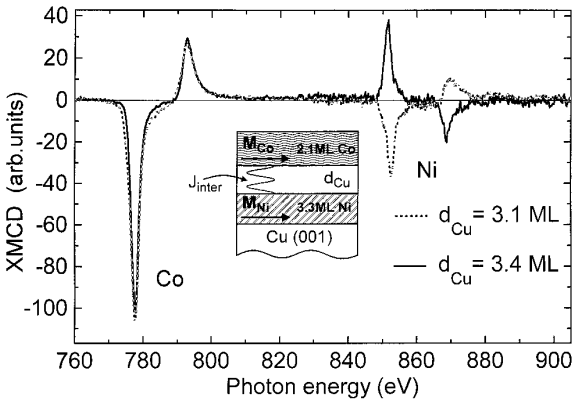

Figure 15. XMCD spectra for Co/Cu/Ni/Cu(001) trilayers. The change of the sign of the Ni spectra above 840 eV for $d_{Cu} = 3.4$ ML indicates the presence of AFM coupling observed for the first time for such thin Cu(001) spacers [114].

[111], by a simple mean field theory: the extra energy introduced in the Ni layer by the interlayer coupling increases its ordering temperature proportionally to J_{inter}. Then, taking into consideration the oscillatory nature of J_{inter} with the spacer thickness d, one would expect a similar oscillation of the increase ΔT_{Ni} with d_{Cu}. Such a behaviour is shown in

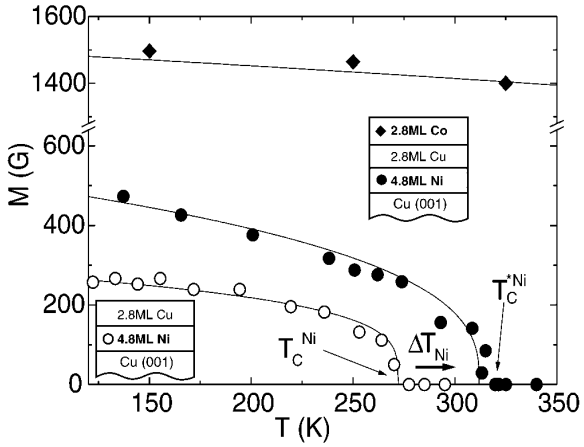

Figure 16. The remanent magnetization of Ni vanishes at about 40 K higher temperature after Co evaporation [114]. Within the experimental sensitivity no magnetic response is observed for temperatures higher than about 310 K.

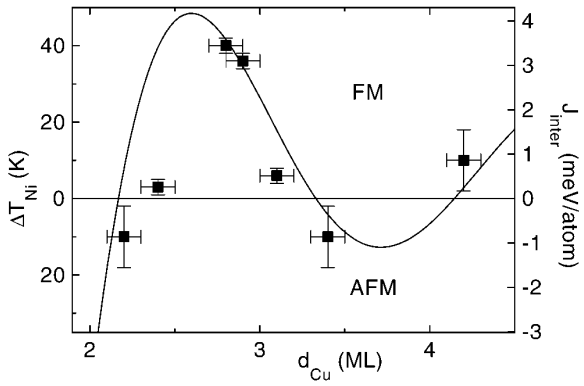

Figure 17. Oscillatory variation of interlayer coupling results in a periodic change of the ordering temperature ΔT_{Ni} in Co/Cu/Ni trilayers [114]. ΔT_{Ni} was measured and J_{inter} was calculated via a molecular field formula which may yield too large values for J_{inter}.

figure 17. The sign of J_{inter} (right Y-axis) was unambiguously determined by XMCD. The sign of ΔT_{Ni} (left Y-axis), however, is always positive, implying that the ordering temperature of Ni is always increasing, independently of the FM or AFM coupling. The solid curve in figure 17 is calculated with the theoretical parameters describing the two periods of oscillation of J_{inter} in an RKKY-like model [112] and their experimental amplitude [113]. Note the excellent agreement between the experimental data points and the theoretical curve without any adjustable parameter [114].

7. Summary

Progress in experimental techniques, *ab initio* calculations and microscopic theories give new insight into thin film magnetism. For the first time experiments on magnetic thin films can provide a complete set of parameters, that is the values of fundamental observables with the film thickness and the temperature to be compared with calculations. MAE is the most important

observable of thin film magnetism, despite the fact that it is a minute fraction of the total energy. MAE is introduced from the point of view of its microscopic origin, that is the anisotropy of the orbital moment. It is demonstrated that by distorting the lattice symmetry we may lift the quenching of the orbital moment in cubic lattices and end up with a huge increase of MAE in the direction perpendicular to the film plane, which is a demand for technology. The T_C of the films can be manipulated by their composition, their thickness (finite-size effect), their structure and the amplitude of interlayer coupling in multilayers. The use of reduced temperatures T/T_C in the study of fundamental observables is stressed. Understanding thin film magnetism is the key to engineer MAE and T_C and it is already giving benefits in terms of technological applications.

Acknowledgments

We would like to thank the members of our group for the experimental work and fruitful discussions: M Farle, A N Anisimov, U Bovensiepen, A Ney, F Wilhelm, W Platow, B Schulz, P Srivastava and M Tischer. E Kosubek is acknowledged for assistance. This work was supported by grant Nos DFG. SFb 290 and BMFB (05SC8 KEA3).

References

[1] Carcia P F, Meinhaldt A D and Suna A 1985 *Appl. Phys. Lett.* **47** 178
[2] Baibich M N, Broto J M, Fert A, Nguyen van Dau F, Petroff F, Eitenne P, Creuzet G, Friederich A and Chazelas J 1988 *Phys. Rev. Lett.* **61** 2472
Grünberg P, Schreiber R, Pang Y, Brodsky M B and Sowers H 1986 *Phys. Rev. Lett.* **57** 2442
[3] Bauer E 1999 *J. Phys.: Condens. Matter* at press
[4] Farle M 1998 *Rep. Prog. Phys.* **61** 755 and references therein
[5] Freeman A J and Wu R 1991 *J. Magn. Magn. Mater.* **100** 497
[6] Gay J G and Richter R 1994 *Ultrathin Magnetic Structures* vol 1, ed J A C Bland and B Heinrich (Berlin: Springer) pp 21–40
Daalderop G H O, Kelly P J and Schurmans M F H *Ultrathin Magnetic Structures* vol 1, ed J A C Bland and M F H Schumans (Berlin: Springer) pp 40–65 and references therein
[7] Hjortstam O, Trygg J, Wills J M, Johansson B and Eriksson O 1996 *Phys. Rev.* B **53** 9204
[8] Szunyogh L, Újfalussy B, Pustogowa U and Weinberger P 1988 *Phys. Rev.* B **57** 8838
Uiberacker C, Zabloudil J, Weiberger P, Szunyogh L and Sommers C 1999 *Phys. Rev. Lett.* **82** 1289
[9] Halilov S V, Perlov A Y, Oppeneer P M, Yaresko A N and Antonov V N 1998 *Phys. Rev.* B **57** 9557
[10] Hjortstam O, Baberschke K, Wills J M, Johansson B and Eriksson O 1997 *Phys. Rev.* B **55** 15 026
[11] Wu R and Freeman A J 1996 *J. Appl. Phys.* **79** 6209
[12] Platow W, Bovensiepen U, Poulopoulos P, Farle M, Baberschke K, Hammer L, Walter S, Müller S and Heinz K 1999 *Phys. Rev.* B **59** 12 641
Müller S, Schulz B, Kostka G, Farle M, Heinz K and Baberschke K 1996 *Surf. Sci.* **364** 235
[13] Heinrich B and Bland J A C 1994 *Ultrathin Magnetic Structures* vol 1, ed Bland J A C and Heinrich B (Berlin: Springer) pp 1–6
[14] Allenspach R 1994 *J. Magn. Magn. Mater.* **129** 160 and references therein
[15] Ferré J, Jamet J P, Pommier J, Beauvillain P, Chappert C, Mégy R and Veillet P 1997 *J. Magn. Magn. Mater.* **174** 77
[16] Bruno P 1999 *J. Phys.: Condens. Matter* at press
[17] Hashimoto S 1994 *J. Appl. Phys.* **75** 438
Krishnan R, Das A, Keller N, Lassri H, Porte M and Tessier M 1997 *J. Magn. Magn. Mater.* **174** L17
[18] Bland J A C and Heinrich B (eds) 1994 *Ultrathin Magnetic Structures* (Berlin: Springer) vols I and II
[19] Wu Te-ho, Hong-Fu, Hajjar R A, Suzuki T and Mansuripur M 1993 *J. Appl. Phys.* **73** 1368
[20] Heinrich B and Cochran J F 1993 *Adv. Phys.* **42** 523
[21] Gradmann U 1991 *J. Magn. Magn. Mater.* **100** 481
Gradmann U 1986 *J. Magn. Magn. Mater.* **54–57** 733

[22] Bloemen P J H, van Alphen E A M, de Jonge W J M and den Broeder F J A 1992 *Math. Res. Soc. Symp. Proc.* vol 231 (Pittsburgh, PA: Materials Research Society) p 479
[23] Anisimov A N, Platow W, Poulopoulos P, Wisny W, Farle M, Baberschke K, Isberg P, Hjörvarsson B and Wäppling R 1997 *J. Phys.: Condens. Matter* **9** 10 581
[24] Zomach M and Baberschke K 1986 *Surf. Sci.* **178** 618
[25] Kawakami R K, Escorcia-Aparicio E J and Qiu Z Q 1996 *Phys. Rev. Lett.* **77** 2570
[26] Anisimov A N, Farle M, Poulopoulos P, Platow W, Baberschke K, Isberg P, Wäppling R, Niklasson A M N and Eriksson O 1999 *Phys. Rev. Lett.* **82** 2390
[27] Platow W, Anisimov A N, Dunifer G L, Farle M and Baberschke K 1998 *Phys. Rev.* B **58** 5611
[28] André G, Aspelmeier A, Schulz B, Farle M and Baberschke K 1995 *Surf. Sci.* **326** 275
[29] Celinski Z, Urquhart K B and Heinrich B 1997 *J. Magn. Magn. Mater.* **166** 6
[30] Stetter U, Aspelmeier A and Baberschke K 1992 *J. Magn. Magn. Mater.* **117** 183
Stetter U, Farle M, Baberschke K and Clark W G 1992 *Phys. Rev.* B **45** 503
[31] Back C H, Würsch C, Kerkmann D and Pescia D 1994 *Z. Phys.* B **96** 1
[32] Bovensiepen U, Poulopoulos P, Farle M and Baberschke K 1998 *Surf. Sci.* **402–404** 396
[33] Poulopoulos P, Farle M, Bovensiepen U and Baberschke K 1997 *Phys. Rev.* B **55** R11 961
[34] Arnold C S, Johnston H L and Venus D 1997 *Phys. Rev.* B **56** 8169
[35] Bader S D 1991 *J. Magn. Magn. Mater.* **100** 440
[36] Berger A, Knappmann S and Oepen H P 1994 *J. Appl. Phys.* **75** 5598
[37] Garreau G, Farle M, Beaurepaire E and Baberschke K 1997 *Phys. Rev.* B **55** 330 and references therein
[38] Ebert H and Schütz G 1996 *Spin-Orbit-Influenced Spectroscopies of Magnetic Solids (Lecture Notes in Physics 466)* (Berlin: Springer)
[39] Chakarian V, Idzerda Y U, Meigs C and Chen C T 1995 *IEEE Trans. Magn.* **31** 3307 and references therein
[40] Aspelmeier A, Tischer M, Farle M, Russo M, Baberschke K and Arvanitis D 1995 *J. Magn. Magn. Mater.* **146** 256
[41] Kittel C 1976 *Introduction to Solid State Physics* (New York: Wiley)
[42] Bruno P 1989 *Phys. Rev.* B **39** 865 Bruno P 1993 *Ferienkurse des Forschungszentrum Jülich* (Jülich: Forschungszentrum Jülich) vol. 24 S.24.1
[43] Recently, van der Laan (van der Laan G 1998 *J. Phys.: Condens. Matter* **10** 3239) has refined Bruno's work ending up with a more sophisticated expression which includes spin-conserved and spin-flip terms between the exchange split majority and minority spin bands, important when the majority band is not completely filled
[44] Abragam A and Bleaney B 1970 *Electron Paramagnetic Resonance of Transition Ions* (Oxford: Clarendon)
[45] Baberschke K 1996 *Appl. Phys.* A **62** 417
[46] Néel L 1954 *J. Physique Radium* **15** 376
[47] Bruno P and Renard J P 1989 *Appl. Phys.* A **49** 499
[48] Chappert C and Bruno P 1988 *J. Appl. Phys.* **64** 5736
[49] Farle M, Mirwald-Schulz B, Anisimov A N, Platow W and Baberschke K 1997 *Phys. Rev.* B **55** 3708
[50] Farle M, Platow W, Kosubek E and Baberschke K *Surf. Sci.* **439** 146
[51] Schulz B and Baberschke K 1994 *Phys. Rev.* B **50**, 13 467
[52] Tischer M, Hjorstam O, Arvanitis D, Hunter Dunn J, May F, Baberschke K, Trygg J, Wills J M, Johansson B and Eriksson O 1995 *Phys. Rev. Lett.* **75** 1602
[53] Weller D, Stöhr J, Nakajima R, Carl A, Samant M G, Chappert C, Megy R, Beauvillain P, Veillet P and Held G A 1995 *Phys. Rev. Lett.* **75** 3752
[54] Andersen O K 1975 *Phys. Rev.* B **12** 3060
Skriver H L 1984 *The LMTO Method* (Berlin: Springer)
[55] Eriksson O, Johansson B, Albers R C, Boring A M and Brooks M S S 1990 *Phys. Rev.* B **42** 2707
Eriksson O, Brooks M S S and Johansson B 1990 *Phys. Rev.* B **41** 7311
[56] Újfalussy B, Szunyogh L, Bruno P and Weinberger P 1996 *Phys. Rev. Lett.* **77** 1805
[57] Wu R, Chen L and Freeman A J 1997 *J. Magn. Magn. Mater.* **170** 103
[58] Callen H B and Callen E R 1966 *J. Phys. Chem. Solids* **27** 1271
[59] Millev Y and Kirschner J 1996 *Phys. Rev.* B **54** 4137
[60] Johnson M T, Bloemen P J H, den Broeder F J A and de Vries J J 1996 *Rep. Prog. Phys.* **59** 1409 and references therein
[61] Angelakeris M, Poulopoulos P, Vouroutzis N, Nyvlt M, Prosser V, Visnovsky S, Krishnan R and Flevaris N K 1997 *J. Appl. Phys.* **82** 5640
[62] Baberschke K and Farle M 1997 *J. Appl. Phys.* **81** 5038
[63] Berghaus A, Farle M, Li Yi and Baberschke K 1990 *Springer Proc. Phys.* **50** 61

[64] Poulopoulos P, Flevaris N K, Krishnan R and Porte M 1994 *J. Appl. Phys.* **75** 4109 and references therein
[65] Louail L, Ounadjela K and Stamps R L 1997 *J. Magn. Magn. Mater.* **167** L189
[66] Schulz B 1995 *PhD Thesis* FU Berlin
[67] Geldart D J W, Hargraves P, Fujiki N M and Dunlap R A 1989 *Phys. Rev. Lett.* **62** 2728 and references therein
[68] Chikazumi S 1966 *Physics of Magnetism* (New York: Wiley) ch 7
[69] Jonker B T, Walker K-H, Kisker E, Prinz G A and Carbonne C 1986 *Phys. Rev. Lett.* **57** 142
[70] Pappas D P, Kamper K-P and Hopster H 1990 *Phys. Rev. Lett.* **64** 3179
[71] Allenspach R and Bischof A 1992 *Phys. Rev. Lett.* **69** 3385
[72] Berger A and Hopster H 1996 *Phys. Rev. Lett.* **76** 519
[73] Jensen P and Bennemann K H 1990 *Phys. Rev.* B **42** 849
[74] Farle M, Platow W, Anisimov A N, Poulopoulos P and Baberschke K 1997 *Phys. Rev.* B **56** 5100
Farle M, Platow W, Anisimov A N, Schulz B and Baberscke K 1997 *J. Magn. Magn. Mater.* **165** 74
[75] Platow W 1999 *PhD Thesis* FU Berlin
[76] Hucht A and Usadel K D 1997 *Phys. Rev.* B **55** 12 309
Hucht A and Usadel K D 1999 *J. Magn. Magn. Mater.* **198/199** 493
Jensen P and Bennemann K H 1998 *Magnetism and Electronic Correlations and Local-Moment Systems: Rare-Earth Elements and Compounds* (Singapore: World Scientific) pp 113–40 and references therein
[77] Herrmann T, Potthoff M and Noltig W 1998 *Phys. Rev.* B **58** 831
[78] Bergholz R and Gradmann U 1984 *J. Magn. Magn. Mater.* **45** 389
[79] Nickel R 1995 *Diploma Thesis* FU Berlin
[80] Tischer M, Arvanitis D, Yokoyama T, Lederer T, Tröger L and Baberschke K 1993 *Surf. Sci.* **307–309** 1096
[81] Schneider C M, Bressler P, Schuster P, Kirschner J, de Miguel J J and Miranda R 1990 *Phys. Rev. Lett.* **64** 1059
[82] Buckley M E, Schumann F O and Bland J A C 1995 *Phys. Rev.* B **52** 6596
[83] May F, Tischer M, Arvanitis D, Hunter Dunn J, Henneken H, Wende H, Chauvistré R and Baberschke K 1997 *J. Physique Coll.* **7** C2 389
[84] Wang D S, Wu R and Freeman A J 1994 *J. Magn. Magn. Mater.* **129** 237
[85] Jensen P J, Dreyssé H and Bennemann K H 1992 *Surf. Sci.* **269/270** 627
[86] Farle M, Lewis W A and Baberschke K 1993 *Appl. Phys. Lett.* **62** 2728
[87] Kerkmann D, Pescia D and Allenspach A 1992 *Phys. Rev. Lett.* **68** 686
[88] Kohlepp J, Elmers H J, Cordes S and Gradmann U 1994 *Phys. Rev.* B **45** 12 287
[89] Li Yi and Baberschke K 1992 *Phys. Rev. Lett.* **68** 1208
[90] Heinz K 1995 *Rep. Prog. Phys.* **58** 637 Heinz K 1999 *J. Phys.: Condens. Matter* at press
[91] Wiesendanger R 1999 *J. Phys.: Condens. Matter* at press
[92] Flevaris N K 1993 *Magnetism and Structure in Systems of Reduced Dimension* ed R F C Farrow *et al* (New York: Plenum) pp 425–438
[93] Aspelmeier A, Gerhardter F and Baberschke K 1994 *J. Magn. Magn. Mater.* **132** 22
[94] Farle M and Baberschke K 1998 *Magnetism and Electronic Correlations in Local-Moment Systems: Rare-Earth Elements and Compounds* (Singapore: World Scientific) pp 35–54
[95] Tober E D, Ynzunza R X, Westphal C and Fadley C S 1996 *Phys. Rev.* B **53** 5444
[96] Zharnikov M, Dittschar A, Kuch W, Schneider C M and Kirschner J 1996 *Phys. Rev. Lett.* **76** 4620
Zharnikov M, Dittschar A, Kuch W, Schneider C M and Kirschner J 1997 *J. Magn. Magn. Mater.* **174** 40
[97] Platow W, Farle M and Baberchke K 1998 *Europhys. Lett.* **43** 713
[98] Berger A, Feldman B, Zillgen H and Wuttig M 1998 *J. Magn. Magn. Mater.* **183** 35
[99] Schmid A K and Kirschner J 1992 *Ultramicroscopy* **42–44** 483
[100] Bovensiepen U, Poulopoulos P, Platow W, Farle M and Baberschke K 1999 *J. Magn. Magn. Mater.* **192** L386
[101] Himpsel F J, Ortega J E, Mankey G J and R F Willis 1998 *Adv. Phys.* **47** 511 and references therein
Johnson P D and Smith 1999 *J. Phys.: Condens. Matter* at press
[102] Fert A, Grünberg P, Barthelemy A, Petroff F and Zinn W 1995 *J. Magn. Magn. Mater.* **140–144** 1 and references therein
[103] Parkin S S P 1999 *J. Phys.: Condens. Matter* at press
[104] Bayreuther G, Bensch F and Kottler V 1996 *J. Appl. Phys.* **79** 4509
[105] Bovensiepen U, Wilhelm F, Srivastava P, Poulopoulos P, Farle M, Ney A and Baberschke K 1998 *Phys. Rev. Lett.* **81** 2368
[106] Wang R W and Mills D L 1992 *Phys. Rev.* B **46** 11 681
[107] Poulopoulos P, Bovensiepen U, Farle M and Baberchke K *J. Magn. Magn. Mater.* submitted
[108] The determination of the coupling sign from the configuration of the sublayer remanent magnetizations is unambiguous for trilayers with small in-plane MAE and large J_{inter}, as are the ones of this work. However, this is not the case for perpendicularly magnetized weakly coupled layers where interesting crossovers may

be recorded; see Poulopoulos P, Bovensiepen U, Farle M and Baberschke K 1998 *Phys. Rev.* B **57** R14 036
[109] Bobo J F, Piecuch M and Snoeck E 1993 *J. Magn. Magn. Mater.* **126** 440
[110] Srivastava P, Wilhelm F, Ney A, Farle M, Wende H, Haack N, Ceballos G and Baberschke K 1998 *Phys. Rev.* B **58** 5701
[111] Actually, the large shift ΔT_{Ni} is a typical feature of the two dimensionality which enlarges the spin fluctuations Jensen P *Phys. Rev.* B, at press
[112] Bruno P and Chappert C 1991 *Phys. Rev. Lett.* **67** 493
[113] Weber W, Allenspach R and Bischof A 1995 *Europhys. Lett.* **31** 491
[114] Ney A, Wilhelm F, Farle M, Poulopoulos P, Srivastava P and Baberschke K 1999 *Phys. Rev.* B **59** R3938